

Enhanced Design of a Floating Broad-band Lossless Tunable HBT Monolithic Active Inductor.

C. Zanchi, T. Parra, L. Escotte, J. Graffeuil.

LAAS-CNRS and Université Paul Sabatier, 7 av. du Colonel Roche, 31077 Toulouse, France.
Tel: (33) 61 33 63 71; Fax: (33) 61 33 69 69

Abstract.

A floating HBT Tunable Active Inductor (TAI) MMIC is reported. Compared with FET circuit, analytical results and measurements show significant improvements over broad-band capability, tunability and selectivity (typical Q 's are over 300). HF noise is also investigated and a minimum noise figure of 0.5 dB is achieved. Measured and simulated results are compared.

I. Introduction.

The monolithic integration of microwave frequency-selective circuits generally suffers from low Q values achieved by passive resonators. To overcome these limitations, grounded [1] or floating active inductors [2] based on GaAs FET technology have been proposed. More recently [3] the design of an HBT active inductor has been reported. It was based on analytical expressions previously derived for FETs. This paper presents an alternative HBT inductor design based on a specific analysis involving some essential intrinsic electrical parameters such as the base-emitter resistance R_{be} . In a first section we analytically demonstrate why HBTs are more convenient than MESFETs for Active Inductor design. In a second section we report the design of an HBT Tunable Active Inductor (TAI) MMIC. Finally experimental results including noise performances are reported and compared with simulated results.

II. Comparison between MESFET and HBT Active Inductors.

Generally, FET Active Inductors are analyzed assuming that the transistor is correctly described in the low frequency range by its gate-to-source capacitance C_{gs} and its transconductance gm . Nevertheless, reference [4] demonstrates the significance of the drain-to-source conductance G_{ds} : at low frequency, an increasing G_{ds} worsens the active inductor performance by increasing its series resistance and by decreasing its equivalent inductance. Consequently, the smaller HBT collector-emitter conductance G_{ce} compared to G_{ds} should improve the inductance characteristics. However, for an HBT, the base-emitter intrinsic resistance R_{be} must also be considered. Indeed, at low frequency, the respective influence of R_{be} and C_{be} may be equivalent. This statement particularly holds true on a standard floating active inductor (fig.1) made of a common-emitter (common-source) cascode configuration (transistors T1, T2), and of a common-base (common-gate) feedback transistor (T3).

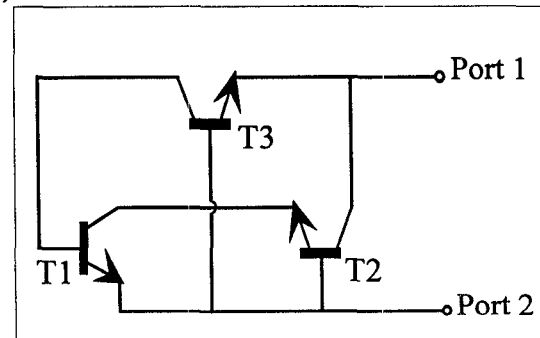


Fig.1 : TAI's circuit configuration.

Preliminary simulations showed that essentially $Gds3$ in the FET device and $Rbe1$ and $Rbe3$ in the HBT circuit have to be considered. The admittance Y seen between port 1 and port 2, is given as:

$$Y = \frac{g_1(gm_3 + G)}{g_1 + G} + g_3 + \frac{gm_1gm_2(gm_3 + G)}{(g_1 + G)(g_2 + gm_2)} \quad (1)$$

where the different parameters value must be taken as:

FET circuit : $G=Gd_3$ and $g=j.Cgs.\omega$

HBT circuit : $G=0$, $g_{1,3}=1/Rbe_{1,3}+j.Cbe_{1,3}.\omega$ and $g_2=j.Cbe_2.\omega$

The corresponding impedance seen between port 1 and 2 can be expressed as:

$$Z = Rs + j.Ls.\omega$$

Under appropriated bias conditions, Rs exhibits a minimum value that can be equal to zero (therefore corresponding to a theoretical infinite Q factor) at a specific frequency f_q expressed by:

$$\text{FET} : f_q = \frac{1}{2\pi} \left(\frac{gm_2 \cdot \sqrt{gm_1 \cdot Gd}}{Cgs_1 \cdot Cgs_2} \right)^{\frac{1}{2}} \quad (2.1)$$

$$\text{HBT} : f_q = \frac{1}{2\pi} \left(\frac{gm_2 \cdot \sqrt{gm_1 \cdot Rbe_1}}{Cbe_1 \cdot Cbe_2 \cdot Rbe_1} \right)^{\frac{1}{2}} \quad (2.2)$$

An operating frequency range in the vicinity of f_q provides the optimum active inductor performance.

To perform a significant comparison between the FET and the HBT circuits, we assume the following assumptions that hold true if the HBTs are conveniently biased:

$$\begin{cases} Cbe \approx 10.Cgs \\ gm(\text{HBT}) \approx 100.gm(\text{FET}) \\ Gd_3 \approx \frac{1}{Rbe_1} \\ f_t(\text{HBT}) = f_t(\text{FET}) \end{cases} \quad (3)$$

where f_t is the transistor cut off frequency.

Using expressions (3) in equations (2.1) and (2.2), shows that the operating frequency f_q ensuring

$Rs=0$ is about 3 times higher using HBTs. Therefore, the HBTs active inductor features an enhanced operating frequency range over FETs. Moreover, considering in (1) that $g_{1,2} \ll gm_{1,2}$ (if $f \ll f_T$), the Q factor can be approximated by:

$$\begin{cases} Q_{\text{FET}} = \frac{Cgs_1 \cdot \omega}{Gd_3} \\ Q_{\text{HBT}} = Rbe_1 \cdot Cbe_1 \cdot \omega \end{cases}$$

Therefore the HBT Active Inductor Q factor is about ten times higher than its FET counterpart.

III. Design of HBT Active Inductors MMICs

Two HBT floating Active Inductor MMICs have been designed. The first one is tunable (TAI) and features two $2\mu\text{m} \times 10\mu\text{m}$ four emitter fingers (T1, T2) for the cascode pair and one $2\mu\text{m} \times 10\mu\text{m}$ single emitter finger (T3) for the feedback (fig.2). The second one is a fixed value active inductor (AI) where a resistor has been substituted for the feedback transistor. The TAI's operating frequency range is 1-10 GHz, and the AI's one is 13-16 GHz. HP MDS software has been used for circuit simulation and layout. The MMICs (useful area is about 0.7 mm^2) were processed by TRW using a $f_t=30$ GHz GaAlAs/GaAs HBT technology.

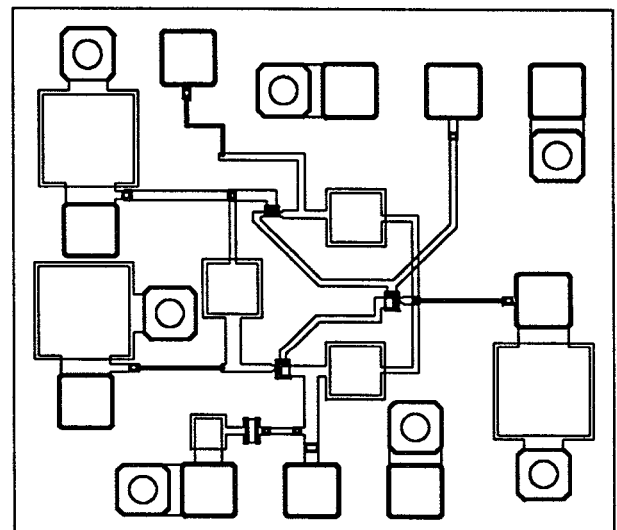


Fig.2 : TAI's MMIC layout.

IV. Electrical performances.

a. Dynamic performance.

Typical on-wafer measurements are displayed on fig.3. The power consumption was about 15 mW. At a 5.7 GHz frequency, the TAI exhibits a 1.7 nH inductance value associated with a 0.1Ω resistance value. Moreover, f_q value can be tuned up to 9.6 GHz by adjusting T1 and T2 bias voltages.

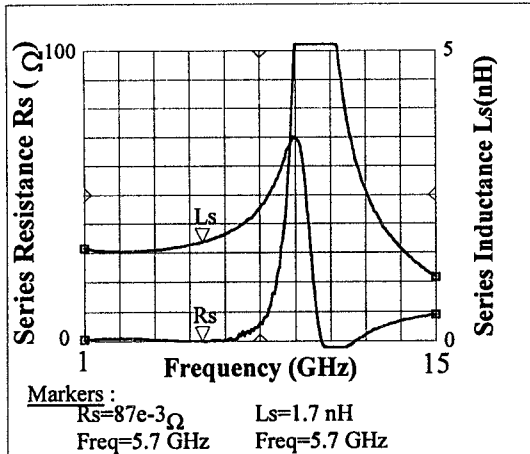


Fig.3 : Measured resistance and inductance versus frequency of the tunable active inductor.

Besides it's broad-band operating frequency, an original feature of the proposed TAI consists in the tuning capabilities of the inductance value. Fig.4 shows the high and low limits of achievable inductance values versus frequency. For instance, at 7 GHz, a 1.4 nH to 4 nH inductance variation range has been obtained under appropriate bias conditions. The series resistance value remains very low ($Rs < 0.5 \Omega$) whatever the inductance value which turns into an enhanced Q factor with a typical value in the range of 300 to 500. All these results validate our theoretical expectations of previous section.

b. Noise performance.

In the operating frequency range, added noise may be a possible drawback of active inductors. To investigate this point, noise parameter measurements were performed on the non tunable AI MMIC.

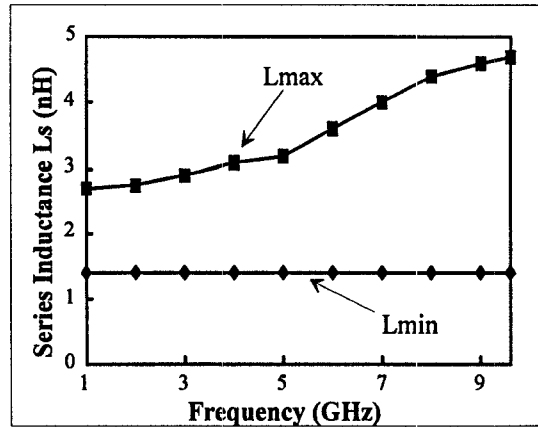


Fig.4 : Upper and lower measured inductance values.

Fig.5 shows the minimum noise figure (F_{min}) and the equivalent noise resistance (R_n) variations versus the series resistance Rs at 14 GHz (the optimum reflection coefficient Γ_{opt} is not shown since it remains constant). A linear decrease of F_{min} and R_n with Rs is observed. With an appropriate input termination, a 0.5 dB minimum noise figure is achieved for a $Rs=0.1 \Omega$ value.

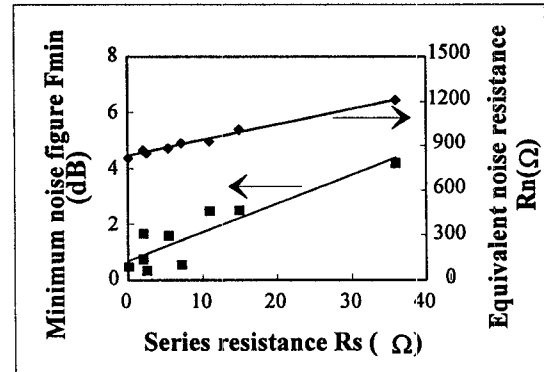


Fig.5 : Measured minimum noise figure and equivalent noise resistance versus the fixed value AI's series resistance.

c. Measurements and simulation comparison.

Subsequently, a dynamic and noise modeling of the AI has been performed, involving, for each transistor, two uncorrelated shot noise current sources ($2qI_b, 2qI_c$) and appropriate thermal noise sources for each of the resistive parts of the circuit. Good agreement between experimental and simulated results is observed for both the AI's series resistance Rs and series inductance Ls (fig.6), and for noise parameters (fig.7). The slight

difference between computed and measured minimum noise figure F_{min} can be attributed to the rough assumption of uncorrelated shot noise sources. Similar results have been observed on the tunable MMIC.

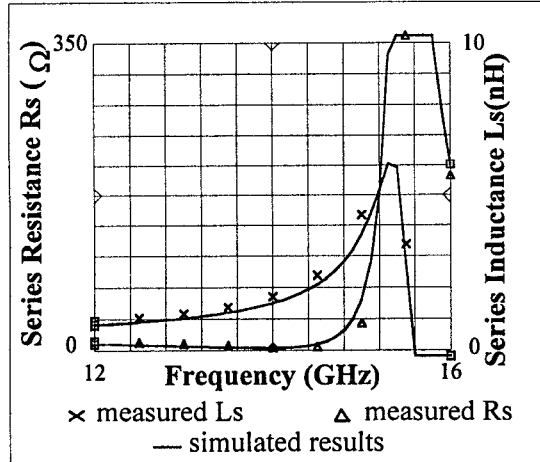


Fig.6 : Measured and simulated resistance and inductance of the fixed value AI.

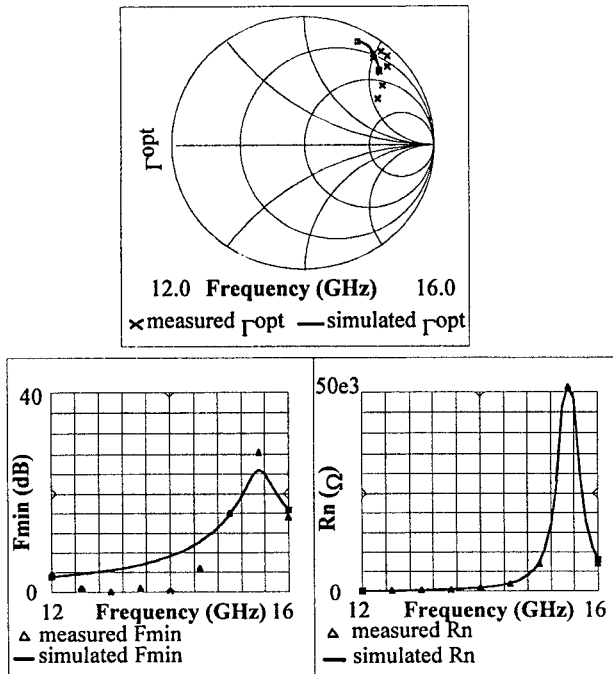


Fig.7 : AI's measured and simulated HF noise parameters.

Therefore we conclude that our HBT active inductor do not exhibit any noise drawback.

V. Conclusion.

An HBT Tunable Active Inductor MMIC has been proposed. Improvements brought by the use of HBT's have been analytically demonstrated and confirmed by measurements. Broad-band capability, tunability and selectivity with additional good HF noise characteristics have been demonstrated and make this circuit attractive for further monolithic integrated filters design.

References.

- [1] S. Hara *et al.*, "Lossless Broad-band Monolithic Microwave Active Inductors", *IEEE Trans. on MTT*, vol.37, N°12, Dec 89.
- [2] G.F Zhang *et al.*, "New Broad-band Tunable Monolithic Microwave Floating Active Inductor", *Electronic letters*, vol.28, Jan.92.
- [3] K.W Kobayashi *et al.*, "A Novel Heterojunction Bipolar Transistor VCO using an Active Tunable Inductance", *IEEE Microwave and guided letters*, vol.4, N°7, July 94.
- [4] R. Kaunisto *et al.*, "Active Inductors for GaAs and Bipolar Technologies", *Analog Integrated Circuits and Signal Processing*, vol.7, pp 35-48, 1995.